



## RESEARCH LETTER

10.1002/2016GL069269

## Key Points:

- The Kramers-Kronig relationship (KKR) for the extensional attenuation and Young's modulus
- An integral form of the nearly local approximation of KKR
- Using KKR for verification of the laboratory measurements of solids at seismic frequencies

## Correspondence to:

V. Mikhailsevitch,  
V.Mikhailsevitch@curtin.edu.au

## Citation:

Mikhailsevitch, V., M. Lebedev, and B. Gurevich (2016), Validation of the laboratory measurements at seismic frequencies using the Kramers-Kronig relationship, *Geophys. Res. Lett.*, *43*, 4986–4991, doi:10.1002/2016GL069269.

Received 25 APR 2016

Accepted 9 MAY 2016

Accepted article online 12 MAY 2016

Published online 27 MAY 2016

## Validation of the laboratory measurements at seismic frequencies using the Kramers-Kronig relationship

Vassily Mikhailsevitch<sup>1</sup>, Maxim Lebedev<sup>1</sup>, and Boris Gurevich<sup>1</sup>

<sup>1</sup>Department of Exploration Geophysics, Curtin University, Perth, Western Australia, Australia

**Abstract** We present a simple procedure concerning the application of the Kramers-Kronig relation for the validation of the laboratory measurements of the extensional attenuation and Young's modulus carried out on the solid specimens at seismic frequencies. The local approximation of the Kramers-Kronig relationship was applied to verify the seismic-frequency measurements conducted on four specimens: a viscoelastic polymethyl-methacrylate (PMMA) sample, and two water- and one glycerol-saturated sandstone samples. The experimental tests were performed at various axial (PMMA sample) and confining (sandstone samples) pressures. The measurements conducted on the PMMA sample and saturated sandstones revealed prominent extensional attenuation and significant dispersion of the Young's modulus. Our analysis shows that the quantitative relationship between the extensional attenuation and the Young's modulus is consistent with the causality principle presented by the Kramers-Kronig relationship. No particular physical models implying any constraints on the physical properties of the samples are required for this validation.

### 1. Introduction

The progress of the modern methods of geophysical exploration is tightly linked to the development of the new effective indicators distinguishing the types of reservoir rocks and fluids. The attenuation and moduli dispersion of a reservoir rock, being direct signs of anelasticity, are an important source of information about the key characteristics of the subsurface interior such as rock composition, permeability, pore fluid properties, and saturation. The numerous theoretical and laboratory studies, which examined the opportunity of using the attenuation and dispersion attributes as indicators of reservoir properties, led to the development of the laboratory techniques and instruments enabling to measure simultaneously elastic moduli and attenuation in the seismic-frequency (SF) range [see, e.g., Jackson and Paterson, 1987; Spencer, 1981; Batzle et al., 2006, Adelinet et al., 2010; Tisato and Madonna, 2012].

One of the central problems that emerge when using the SF devices is the acoustic resonances occurring in the mechanical parts of the devices, which overlap and distort the signals obtained from the sample [Adam et al., 2009]. The solution of this problem requires a diagnostic instrument to validate the quality of experimental data, which would be able to corroborate the physical nature of the detected signals, in other words, monitor the artefacts caused by uncontrolled experimental conditions. Considering that the measurements of attenuation and elastic moduli are independent and take place in the same frequency range, it appears natural to use the consistency of the experimental data with the causality principle as a quality control measure.

Mathematically, the causality principle is often expressed through Kramers-Kronig equations, which link real and imaginary parts of a complex function that controls wave propagation in medium, such as a complex wave number or a complex elastic modulus. For acoustic waves, a convenient approximate form of Kramers-Kronig relations (KKR) was found by O'Donnel et al. [1978], who derived an expression linking a phase velocity with attenuation at a specific frequency, which was successfully used for validating the results of the ultrasonic experiments conducted on hemoglobin solutions. Later, O'Donnel et al. [1981] presented a model of attenuation for the class of loss mechanisms associated with relaxational phenomena, which was applied to validate the ultrasonic data obtained for materials exhibiting relaxation such as polyethylene and CoSO<sub>4</sub>-water solution. A relaxation model with a Cole-Cole distribution of relaxation times was used by Spencer [1981] for verification of the attenuation and Young's modulus dispersion measurements carried out on liquid-saturated sandstone, limestone, and granite at seismic frequencies. Dvorkin and Mavko [2006] developed a model of the attenuation estimation based on the standard linear solid approximation that links the attenuation to the corresponding elastic modulus.

It should be noted that the attenuation models elaborated in *O'Donnel et al.* [1981] and *Spencer* [1981] and *Dvorkin and Mavko* [2006] are based on assumptions of the physical properties of materials which go beyond the casualty principle and have a restricted area of application.

The aim of this paper is to illustrate the applicability of KKR for validating the data obtained in SF experiments. It is shown that for the subresonance type of SF measurements, the relation between the measured Young's modulus and extensional attenuation can be verified using an approximation of KKR, whereby the reliability of SF tests might be significantly enhanced. We emphasize that no assumption about the physical characteristics of materials is necessary for this validation.

## 2. Kramers-Kronig Relation for the Young's Modulus

Let us consider an isotropic viscoelastic material regarded as a dynamic system for which the stress-strain relationship is linear and whose mechanical property is characterized by the complex Young's modulus

$$E^*(\omega) = \frac{\sigma}{\varepsilon} = |E^*(\omega)| \exp(i\varphi(\omega)) = E_m (\cos \varphi + i \sin \varphi) = E'(\omega) + iE''(\omega), \quad (1)$$

where  $E_m = |E^*(\omega)|$  is the absolute magnitude of the Young's modulus  $E^*$ ; the real  $E'$  and imaginary  $E''$  parts of  $E^*$  are the storage and loss moduli, correspondingly;  $\varphi(\omega)$  is the phase angle between the force applied to the sample and its displacement (loss angle), and  $\omega = 2\pi f$ ,  $f$  is the frequency of the periodical stress  $\sigma$ . *Christensen* [1982] showed that if the imaginary part  $E''$  is slowly changing with respect to frequency, the nearly local approximation of the integral Kramers-Kronig equations relating the loss modulus  $E''$  at a specific frequency  $\omega$  to the local frequency derivative of the storage modulus  $E'$  takes the form

$$E''(\omega) = \frac{\pi}{2} \omega \frac{dE'(\omega)}{d\omega}. \quad (2)$$

Taking into account that the extensional attenuation defined as the inversed quality factor  $Q_E^{-1}$  and the phase angle  $\varphi(\omega)$  are connected by the relation

$$Q_E^{-1} = \frac{E''}{E'} = \tan(\varphi), \quad (3)$$

and dividing both parts of equation (2) by  $E'(\omega)$ , we find the relationship connecting attenuation  $Q_E^{-1}$  and storage modulus  $E'(\omega)$ :

$$Q_E^{-1} = \frac{\pi}{2} \frac{\omega}{E'(\omega)} \frac{dE'(\omega)}{d\omega}, \quad (4)$$

which yields the expression for  $E'$  at a frequency  $f$

$$E'(f) = E'_0 \exp \left[ \frac{2}{\pi} \int_{f_0}^f \frac{Q_E^{-1}}{f'} df' \right]. \quad (5)$$

Taking into account that modulus dispersion and attenuation are usually considered on a logarithmic frequency scale, equation (5) can be transformed to

$$E'(f) = E'_0 \exp \left[ \frac{2}{\pi \lg(e)} \int_{\lg(f_0)}^{\lg(f)} Q_E^{-1} d \lg(f') \right] \approx E'_0 \exp \left[ 1.466 \int_{\lg(f_0)}^{\lg(f)} Q_E^{-1} d \lg(f') \right], \quad (6)$$

where  $e$  is Euler's number,  $\lg$  is the decimal logarithm, and  $E'_0$  is the storage modulus measured at some reference frequency  $f_0$ .

If the magnitude of attenuation is small  $Q_E^{-1} \ll 1$ , equations (3) and (6) can be simplified to

$$Q_E^{-1} \approx \varphi, \quad (7)$$

and

$$E'(f) = E'_0 + 1.466 E'_0 \int_{\lg(f_0)}^{\lg(f)} \varphi d \lg(f'). \quad (8)$$

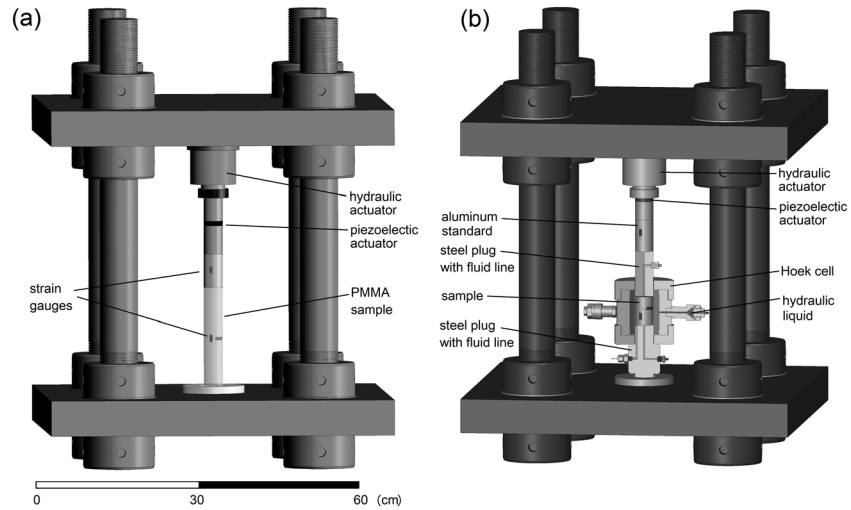


**Figure 1.** Two versions of the seismic-frequency laboratory rig: with the (a) uniaxial and (b) confining static pressures applied to a specimen.

Equations (5), (6), and (8) connect the attenuation and storage modulus and can be used for verification of the SF experimental data. Equations (7) and (8) are strikingly simple and allow visual check of causality by comparing the behavior of the storage modulus and phase angle. However, for calculations it is more accurate to use the full expressions (5) or, equivalently, (6).

It should be pointed out that the relationships identical with equation (2) were also derived for imaginary and real parts of two other commonly used characteristics of viscoelastic materials: complex compressibility [O'Donnel *et al.*, 1978, 1981] and complex shear modulus [Booij and Thoone, 1982].

### 3. Experimental Setup

In this study we used two versions of the SF apparatus, with and without confining pressure, which measures the Young's modulus and extensional attenuation of a specimen at strain magnitudes of  $10^{-8}$  to  $10^{-6}$  (Figure 1).

For the measurements on the polymethyl-methacrylate (PMMA) sample, we used the simplified uniaxial configuration presented in Figure 1a, when for the tests carried out on the sandstone samples, we used the configuration comprising the Hoek triaxial cell as it is shown in Figure 1b. The detailed description of the SF apparatus and its operation is presented in Mikhaltsevitch *et al.* [2014].

### 4. Samples and Experimental Procedure

We apply equation (8) to the experimental data obtained at seismic frequencies for four specimens: a cylindrical viscoelastic PMMA sample, two low-permeability sandstone samples retrieved from the regions of Donnybrook and Harvey, Western Australia, and one Berea sandstone sample. The parameters of the PMMA sample, which for convenience is designated as sample A, are length—150.0 mm, diameter—38.0 mm, and density—1185 kg/m<sup>3</sup>. The petrophysical parameters of the samples, which we denote as samples B (Donnybrook), C (Harvey), and D (Berea), are presented in Table 1.

The Young modulus  $E$  is determined as follows. The periodic stress  $\sigma_{zz}$  provided by the multilayer piezoelectric actuator can be expressed as

$$\sigma_{zz} = E_{st} \epsilon_{zz}^{st} / \epsilon_{zz}, \tag{9}$$

where  $\epsilon_{zz}^{st}$  and  $\epsilon_{zz}$  are the amplitudes of the longitudinal strains measured in the standard and specimen, correspondingly, and  $E_{st}$  is the Young's modulus of the standard. Therefore, the Young's modulus  $E$  is

$$E = E_{st} \epsilon_{zz}^{st} / \epsilon_{zz}. \tag{10}$$

**Table 1.** Petrophysical Data for the Sandstone Samples

Sample	B (Donnybrook)	C (Harvey)	D (Berea)
Porosity, %	14.8	18.0	19.0
Helium permeability, $\times 10^{-15} \text{ m}^2$ (mD)	7.7 (7.8)	9.5 (9.6)	
Water permeability, $\times 10^{-15} \text{ m}^2$ (mD)	0.7 (0.7)	1.1 (1.1)	
Glycerol permeability, $\times 10^{-15} \text{ m}^2$ (mD)			71 (72)
Density, $\text{kg/m}^3$	2099	2110	2080
Length, mm	70	72	70
Diameter, mm	38	38	38
Quartz, %	62	73	80
Feldspar, %		11	12
Microcline, %	15		
Calcite, %		3	
Albite, %	6		
Kaolinite, %	17	13	8
Mineral bulk modulus, GPa	30.9	32.3	32.0

In our measurements the attenuation  $Q_E^{-1}$  is found as a phase angle  $\phi$  between the force applied to the sample and its displacement [O'Connell and Budiansky, 1977].

The experimental procedure in our study was as follows. Sample A was measured at axial pressures of 7 and 15 MPa; no lateral pressure was applied. Sandstone samples B, C, and D were measured in dry and liquid-saturated states. The sandstones were saturated with deionized water (samples B and C) and glycerol (sample D). The measurements on sample B in dry and saturated states were performed at confining pressures of 2.5, 7, and 15 MPa and an ambient pore pressure (~0.1 MPa). Dry sample C was measured at confining pressures of 9 MPa and 23 MPa and an ambient pore pressure. The measurements for water-saturated sample C were performed at confining pressures of 15 MPa and 29 MPa and a pore pressure of 6 MPa, so the differential pressure (confining pressure minus pore pressure) was unchanged. The SF experiments with the samples B and C were carried out at room temperature (22°C). Dry sample D was tested at a confining pressure of 10 MPa and an ambient pore pressure under a temperature of 23°C. The measurements on glycerol-saturated sample D were carried out at a confining pressure of 13 MPa and a pore pressure of 3 MPa under temperatures of 23, 31, and 37.5°C. The frequency range of the periodic stress used in the tests was 0.1–100 Hz for samples A and B, 0.1–120 Hz for sample C, and 0.01–100 Hz for sample D. The number of signal averages in our experiments was 100.

### 5. Experimental Results

The experimental results obtained for all samples are presented in Figures 2–5. The error bars for the moduli estimates were computed in accordance with the uncertainty analysis procedure developed for SF measurements in Adam et al. [2009]. The dependences of the extensional attenuation and Young's modulus on frequency of the sinusoidal stress applied to sample A obtained for two static axial pressures are presented in Figure 2. In Figures 3 and 4 one can see the results of the attenuation and Young's modulus measurements carried out on sandstones B

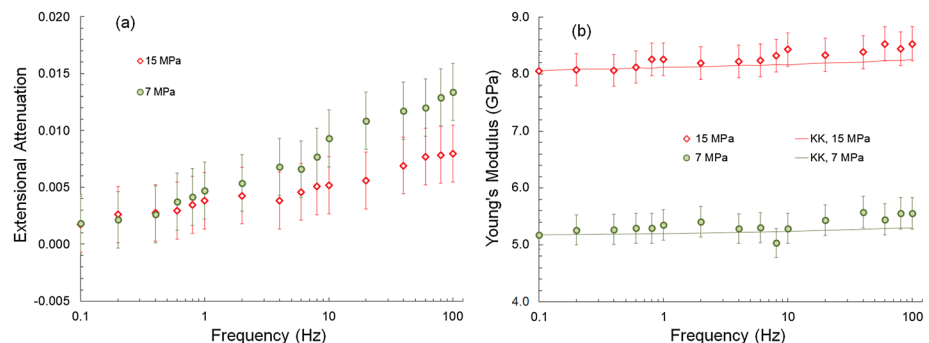


**Figure 2.** The (a) attenuation  $Q_E^{-1}$  and (b) Young's modulus measured and computed using KKR for sample A at two axial pressures of 15 and 7 MPa.

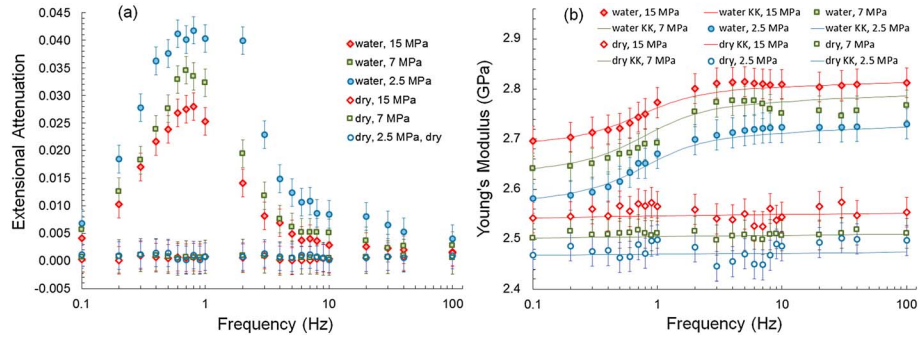


**Figure 3.** The (a) attenuation  $Q_E^{-1}$  and (b) Young's moduli measured and computed using KKR for sample B. The confining pressures are 2.5 and 15 MPa in dry state and 2.5, 7, and 15 MPa in water-saturated state. The pore pressure is ambient for both dry and saturated states.

and C under dry and water-saturated conditions, respectively. The results of the measurements on dry and glycerol-saturated sample D are shown in Figure 5.

Let us note that the attenuation and dispersion observed in sample A represent a typical behavior of acrylic plastic in the seismic frequency range [Spencer, 1981; Tisato and Madonna, 2012]. The physical nature of the attenuation and modulus dispersion observed in samples B, C, and D was discussed previously in our publications [Mikhaltsevitch et al., 2013, 2015] and is beyond the scope of this paper.

### 6. Calculation of Dispersion from Attenuation

The simplest approximation of equation (6) suitable for computing the dependence of the storage modulus  $E'(f)$  from attenuation data can be presented in the form

$$E'(f_L) = E'_0 \exp \left[ 0.733 \sum_{i=1}^{L-1} (\varphi_{i+1} + \varphi_i) \lg(f_{i+1}/f_i) \right]. \quad (11)$$

Here  $L$  is the number of the measurement frequencies  $f_i$  corresponding to the number of the measured stress-strain phase angles  $\varphi_i$ .

More accurate approximation can be achieved using cubic splines for data interpolation (see, e.g., Yang et al. [2005]) as

$$E'(f_M) = E'_0 \exp \left[ 0.733 \sum_{k=1}^{M-1} (\tilde{\varphi}(f_{k+1}) + \tilde{\varphi}(f_k)) \lg(f_{k+1}/f_k) \right], \quad (12)$$

where  $M$  is the number of the breakpoints chosen for the spline interpolation and  $\tilde{\varphi}$  is the cubic spline function used for the interpolation of a given set of the measured phase values  $\varphi_i$  ( $i=1 \dots L$ ) at a frequency of  $f_k$  ( $k=1 \dots M$ ).

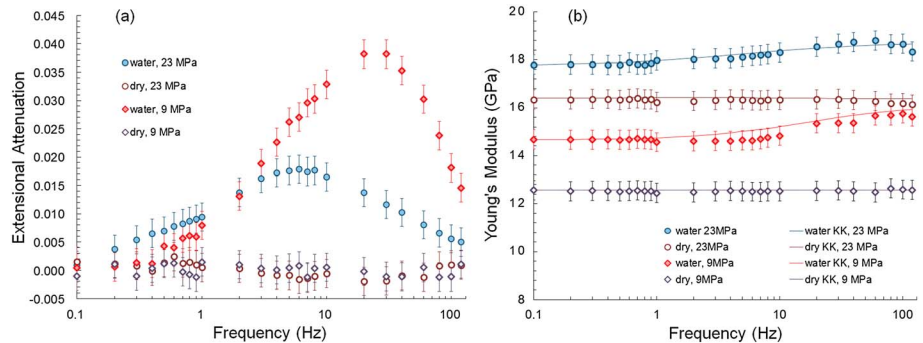


**Figure 4.** The frequency dependencies of (A) the attenuation  $Q_E^{-1}$  and (B) Young's moduli measured and computed using KKR for the sample C in dry and water-saturated conditions at two confining pressures of 9 MPa and 29 MPa; the pore pressure is ambient in dry state and 6 MPa under saturated conditions.

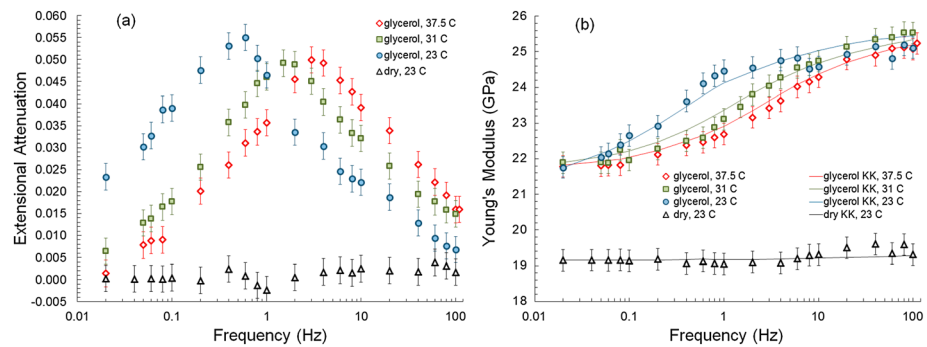


**Figure 5.** The dependencies on frequency for (A) the attenuation  $Q_E^{-1}$  and (B) Young's moduli of sample C measured in dry and glycerol-saturated states. The differential pressure is 10 MPa in both dry and saturated states. The Young's moduli computed using KKR are indicated by the dash lines. The measurements on the glycerol-saturated sample were conducted at 23, 31, and 37.5°C.

Using equation (12), we have computed the dependences of the Young's modulus from attenuation data. The results of numerical integration, presented in Figures 2b–5b, demonstrate a good match between the dependences of the measured Young's moduli and Young's moduli computed using KKR. Thus, we conclude that the attenuation and dispersion measurements are consistent with the causality principle. This indicates that the dispersion and attenuation have a common physical source.

### 7. Conclusions

In this paper we present a method relating to the application of the Kramers-Kronig relation for verification of the laboratory measurements of the extensional attenuation and Young's modulus carried out on the solid specimens at seismic frequencies. The method was applied to the results of the SF tests conducted on a set of samples comprising a viscoelastic PMMA sample, two sandstone samples excavated in Donnybrook and Harvey, Western Australia, and one Berea sandstone sample. The measurements on the sandstones were performed under dry, water- (Donnybrook and Harvey), and glycerol-saturated (Berea) conditions. It was demonstrated that the quantitative relationship between the extensional attenuation and frequency dependence of the Young's modulus measured for the PMMA sample and all sandstones is consistent with the causality principle expressed by the Kramers-Kronig relationship.

### Acknowledgments

Authors acknowledge the financial support provided by the Curtin Reservoir Geophysical Consortium. Excel files with data are available at [https://www.dropbox.com/s/11986nyxnskbnj/KK\\_data.rar?dl=0](https://www.dropbox.com/s/11986nyxnskbnj/KK_data.rar?dl=0)

### References

Adam, L., M. Batzle, K. T. Lewallen, and K. van Wijk (2009), Seismic wave attenuation in carbonates, *J. Geophys. Res.*, *114*, B06208, doi:10.1029/2008JB005890.

Adelinet, M., J. Fortin, Y. Gueguen, A. Schubnel, and L. Geoffroy (2010), Frequency and fluid effects on elastic properties of basalt: Experimental investigations, *Geophys. Res. Lett.*, *37*, L02303, doi:10.1029/2009GL041660.

Batzle, M., D. Han, and R. Hofmann (2006), Fluid mobility and frequency-dependent seismic velocity: Direct measurements, *Geophysics*, *71*(1), N1–N9, doi:10.1190/1.2159053.

Booij, H. C., and G. P. J. M. Thone (1982), Generalization of Kramers-Kronig transforms and some approximations of relations between viscoelastic quantities, *Rheol. Acta*, *21*(1), 15–24, doi:10.1007/BF01520701.

Christensen, R. M. (1982), *Theory of Viscoelasticity: An Introduction*, Academic Press, New York.

Dvorkin, J. P., and G. Mavko (2006), Modeling attenuation in reservoir and nonreservoir rock, *Leading Edge*, *25*, 194–197, doi:10.1190/1.2172312.

Jackson, I., and M. S. Paterson (1987), Shear modulus and internal friction of calcite rocks at seismic frequencies: Pressure, frequency and grain size dependence, *Phys. Earth Planet. Inter.*, *45*(4), 349–367, doi:10.1016/0031-9201(87)90042-2.

Mikhailtsevitch, V., M. Lebedev, and B. Gurevich (2013), An experimental study of low-frequency wave dispersion and attenuation in water saturated sandstones, *Poromechanics V: Proc. Fifth Biot Conf. Poromechanics*, 135–144, doi:10.1061/9780784412992.016.

Mikhailtsevitch, V., M. Lebedev, and B. Gurevich (2014), A laboratory study of the elastic and anelastic properties of the sandstone flooded with supercritical CO<sub>2</sub> at seismic frequencies, *Energy Procedia*, *63*, 4289–4296, doi:10.1016/j.egypro.2014.11.464.

Mikhailtsevitch, V., M. Lebedev, and B. Gurevich (2015), A laboratory study of attenuation and dispersion effects in glycerol-saturated Berea sandstone at seismic frequencies, in *2015 SEG Annual Meeting*, New Orleans, 3085–3089, doi:10.1190/segam2015-5898429.1.

O'Connell, R. J., and B. Budiansky (1977), Viscoelastic properties of fluid-saturated cracked solids, *J. Geophys. Res.*, *82*, 5719–5740, doi:10.1029/JB082i036p05719.

O'Donnel, M., E. T. Jaynes, and J. G. Miller (1978), General relationships between ultrasonic attenuation and dispersion, *J. Acoust. Soc. Am.*, *63*(6), 1935–1937, doi:10.1121/1.381902.

O'Donnel, M., E. T. Jaynes, and J. G. Miller (1981), Kramers-Kronig relationship between ultrasonic attenuation and phase velocity, *Acoust. Soc. Am.*, *69*(3), 696–701, doi:10.1121/1.385566.

Spencer, J. W. (1981), Stress relaxation at low frequencies in fluid-saturated rocks: Attenuation and modulus dispersion, *J. Geophys. Res.*, *86*, 1803–1812, doi:10.1029/JB086iB03p01803.

Tisato, N., and C. Madonna (2012), Attenuation at low seismic frequencies in partially saturated rocks: Measurements and description of a new apparatus, *J. Appl. Geophys.*, *86*, 44–53, doi:10.1016/j.jappgeo.2012.07.008.

Yang, W. Y., W. Cao, and J. Morris (2005), *Applied Numerical Methods Using Matlab*, John Wiley, Hoboken, N. J.